MOLECULAR AND CELLULAR BIOLOGY, May 2009, p. 2359–2371 Vol. 29, No. 9
0270-7306/09/$08.00+0 doi:10.1128/MCB.01259-08

Polycystin-1 Regulates Extracellular Signal-Regulated Kinase-Dependent Phosphorylation of Tuberin To Control Cell Size through mTOR and Its Downstream Effectors S6K and 4EBP1▽

Gianfranco Distefano,[1] Manila Boca,[1] Isaline Rowe,[1] Claas Wodarczyk,[1] Li Ma,[2] Klaus B. Piontek,[3] Gregory G. Germino,[3] Pier Paolo Pandolfi,[4,5] and Alessandra Boletta[1]*

Dulbecco Telethon Institute at Dibit-San Raffaele, Milan, Italy[1]; Whitehead Institute for Biomedical Research, Cambridge, Massachusetts[2]; The Johns Hopkins University School of Medicine, Baltimore, Maryland[3]; Harvard Medical School, Boston, Massachusetts[4]; and Beth Israel Deaconess Medical Center, Boston, Massachusetts[5]

Received 8 August 2008/Returned for modification 12 August 2008/Accepted 6 February 2009

Autosomal dominant polycystic kidney disease (ADPKD) is a common genetic disease characterized by bilateral renal cyst formation. Both hyperproliferation and hypertrophy have been previously observed in ADPKD kidneys. Polycystin-1 (PC-1), a large orphan receptor encoded by the *PKD1* gene and mutated in 85% of all cases, is able to inhibit proliferation and apoptosis. Here we show that overexpression of PC-1 in renal epithelial cells inhibits cell growth (size) in a cell cycle-independent manner due to the downregulation of mTOR, S6K1, and 4EBP1. Upregulation of the same pathway leads to increased cell size, as found in mouse embryonic fibroblasts derived from *Pkd1*$^{-/-}$ mice. We show that PC-1 controls the mTOR pathway in a Tsc2-dependent manner, by inhibiting the extracellular signal-regulated kinase (ERK)-mediated phosphorylation of tuberin in Ser664. We provide a detailed molecular mechanism by which PC-1 can inhibit the mTOR pathway and regulate cell size.

Autosomal dominant polycystic kidney disease (ADPKD) is one of the most common genetic diseases, affecting about 1 in 1,000 individuals (38). The disease can be caused by mutations in either *PKD1*, accounting for 85% of cases, or *PKD2*, accounting for the remaining 15% of cases. Mutations in these two genes give rise to the same undistinguishable phenotype characterized by bilateral renal cyst formation. The disease is, however, systemic, with several other organs affected. In particular, 10% and 80% of patients develop cysts in the pancreas and liver, respectively (38).

The functions of the two proteins generated by the *PKD1* (polycystin-1 [PC-1]) and *PKD2* (PC-2) genes are slowly being unraveled. The first is a large plasma membrane, non-tyrosine kinase receptor whose ligand remains elusive. It is believed to play a role in cell-cell/matrix interactions, where the long extracellular domain can homodimerize (15) and could thus serve as a ligand. PC-1 might also be functioning as a mechanosensor on the primary cilium or at cell-cell junctions (6). PC-1 interacts through an intracellular coil-coiled domain with PC-2, a nonselective cation channel with a preference for calcium, and regulates its channel activity (6, 13, 28). The PC-1/PC-2 complex can regulate a number of different biological processes including cell proliferation, apoptosis, cell migration, and tubulogenesis (2–5, 22). Here we investigated the role of PC-1 in controlling cell growth (size) in addition to proliferation.

Cell growth is the process regulating an increase in cell mass in response to a number of extracellular signals, including nutrient availability and growth factors, and it is distinct from cell proliferation, though the two are interconnected (8). The precise mechanism allowing cells to reach and maintain their final size is not completely understood, but one important pathway regulating this process is the mTOR (mammalian target of rapamycin) cascade (27, 31, 40). mTOR is a serine/threonine kinase involved in regulating cell cycle progression, translational control, ribosomal biogenesis, and cellular energy responses (37). Its capability to regulate cell size in mammals has been attributed mainly to its capability to regulate two downstream effectors: S6K (p70S6K), a Ser/Thr kinase initially identified as the kinase responsible for phosphorylating the ribosomal subunit protein S6, and 4EBP1 (eukaryotic initiation factor 4E-binding protein 1), which represses translation by associating with eIF4E (9). Activation of the mTOR pathway results in increased phosphorylation of S6K and 4EBP1, and the cooperation between these two pathways results in increased cell size due to enhanced translation and increased proliferation (9, 31).

The details of how mTOR can be activated are still unknown, but it has been demonstrated to require Rheb, a small GTPase of the Ras superfamily. When Rheb is in its active state (GTP bound), it is able to induce mTOR kinase activity (40). The guanine nucleotide exchange factor-inducing Rheb active state might have been recently identified (14), while the GTPase-activating protein responsible for inducing its inactive state has been identified as the *TSC2* gene product, tuberin (36). *TSC2* is one of the two genes mutated in tuberous sclerosis, a genetic disease characterized by seizures, hamartomas in several organs, and renal cystic disease. The second gene mutated in tuberous sclerosis, *TSC1*, encodes hamartin, an important cofactor of tuberin. The fine regulation of the tuberin/hamartin complex has recently been the matter of in-

* Corresponding author. Mailing address: Dulbecco Telethon Institute at Dibit-San Raffaele, Via Olgettina 58, 20132 Milan, Italy. Phone: 39-02 2643 4805. Fax: 39-02 2643 4861. E-mail: boletta.alessandra@hsr.it.

▽ Published ahead of print on 2 March 2009.

tense studies in mammalian cells, and several mechanisms of regulation have been described, highlighting the complexity of this regulation. Tuberin can be phosphorylated at at least nine distinct phospho-sites (1). Several kinases have been reported to phosphorylate and regulate tuberin, including Akt (7, 25), p90RSK (30), the extracellular signal-regulated kinases (ERKs) (24), and AMPK (17).

Three recent reports have shown that the mTOR pathway is upregulated in several mouse models of polycystic kidney disease in which rapamycin is able to inhibit cyst expansion (33, 35, 39). Furthermore, Shillingford et al. have reported that a short portion of the C-tail of PC-1 interacts with Tsc2 (33). Although the role of this interaction in regulating downstream pathways was not investigated, it was hypothesized that somehow PC-1 might be able to inhibit the mTOR pathway through this interaction.

Here we show that PC-1 regulates the mTOR pathway and, subsequently, cell growth (size), in addition to regulating proliferation. Furthermore, we show that PC-1 is able to control the ERK-dependent phosphorylation of tuberin, resulting in the downregulation of mTOR and its downstream targets p70S6K and 4EBP1. Surprisingly, even if PC-1 induces Akt activation, this alone is unable to achieve activation of the Tsc2/mTOR pathway.

Our data provide molecular insight into how PC-1 regulates the mTOR pathway, which is potentially relevant for both understanding ADPKD pathogenesis and designing therapeutic approaches.

MATERIALS AND METHODS

Antibodies, reagents, and inhibitors. Anti-P-Ser473-Akt, anti-P-Thr389-p70S6K, anti-P-Ser235/236-S6Rp, anti-P-Thr1472-tuberin, anti-P-Ser939-tuberin, anti-P-MEK, anti-P-ERK, anti-P-p90RSK, anti-S6Rp, anti-Akt, anti-Tsc2, and anti-ERK antibodies were from Cell Signaling Technologies. Antituberin (C-20, sc-893), anti-p70S6K (C-18, sc-230), and anti-PC-1 (C-20, sc-10372, lot no. K2800) were from Santa Cruz. The high-affinity antihemagglutinin (anti-HA) antibody was from Roche (catalog no. 1867423).

U0126 and rapamycin (Cell Signaling Technologies) were employed at final concentrations of 30 μM and 25 nM, respectively.

Western blot analysis. For Western blot analysis, the cells were lysed (lysis buffer: 250 mM sucrose, 20 mM imidazole, 1 mM EDTA, pH 7.4, and 0.5% Triton X-100, supplemented with protease inhibitor cocktail [Amersham] and phosphatase inhibitors [1 mM final concentration of glycerophosphate, sodium orthovanadate and sodium fluoride]). Total lysates were quantified, and Laemmli buffer was added to reach a 1× final concentration. Proteins were resolved in a sodium dodecyl sulfate-polyacrylamide gel electrophoresis gel and transferred onto polyvinylidene difluoride membranes. Next, 5% milk in Tris-buffered saline–Tween 20 was used for blocking and for secondary antibody incubations, while 2% bovine serum albumin in TBS-T was used for incubations with primary antibodies. Horseradish peroxidase-conjugated secondary antibodies (from Roche) were visualized using an ECL system (Amersham), and they were mixed with a Super-Femto ECL system from Pierce when necessary. Quantification of the Western blots was performed using the program ImageQuant.

FACS analysis of cell size, cell cycle, and phosphorylation of ERKs and S6Rp. Cells were trypsinized and centrifuged for 5 min at 1,200 rpm, and then the pellets were resuspended in 1 ml of phosphate-buffered saline (PBS). Fluorescence-activated cell sorter (FACS) analysis (FACScan; Becton Dickinson) was performed, and the mean forward scatter height (FSC-H) was determined. For cell cycle analysis, cells were washed once with PBS, trypsinized, and centrifuged for 5 min at 1,200 rpm. Pellets were resuspended in 1 ml of buffer solution (1.10 g/liter glucose, 8.00 g/liter NaCl, 0.40 g/liter KCl, 0.20 g/liter Na_2HPO_4, 0.15 g/liter KH_2PO_4, and 0.20 g/liter EDTA) and fixed by adding 3 ml of 100% ethanol (75% final concentration). Immediately before analysis, cells were centrifuged at 1,500 rpm for 5 min, washed once with PBS, and incubated at room temperature for 1 h in 500 μl of a staining solution (25 μg/ml of propidium iodide [PI], 1 mg/ml of RNase A, 40 μl of Nonidet [1%], and 0.1% sodium citrate). Cell cycle histograms were generated after analysis of the PI-stained cells with a Becton Dickinson FACScan. For each sample, at least 1×10^4 events were recorded. Single cells were gated away from clumped cells using an FL2 width versus FL2 area dot plot. To quantitatively measure the percentage of cells in the various phases of the cell cycle, the "marker tool" of the CellQuest Pro or FlowJo software was used to gate the G_0/G_1-, S-, and G_2/M-phase peaks. The mean FSC-H was determined on the G_0/G_1, S, and G_2/M gated cells identified by PI fluorescence.

For the analysis of phospho-ERK and phospho-S6Rp, cells were fixed in PBS with 2% formaldehyde for 10 min at 37°C, washed twice in PBS, permeabilized in 1 ml ice-cold PBS with 90% methanol, and washed twice and stained with 1:100 pERK or pS6Rp (Cell Signaling Technology) antibody in a PBS and 4% fetal calf serum (FCS) solution for 15 min at room temperature. Cells were washed twice in PBS with 4% FCS, resuspended in 100 μl of PBS with 4% FCS, and incubated with 1 μl of Alexa Fluor 488 secondary antibody (catalog no. A21441; Molecular Probes, Invitrogen). For DNA labeling, the cells were stained with 100 μl of PBS with 10 μg/ml DAPI (4′,6′-diamidino-2-phenylindole, sc-3598; Santa Cruz). Cell cycle histograms were generated after analysis of the DAPI-stained cells with a Becton Dickinson FACS CANTO instrument. For each sample, at least 1×10^4 single cells were gated away from the clumped cells using a Pacific Blue width versus Pacific Blue area dot plot. The mean FSC-H was determined on the G_0/G_1, S, and G_2/M gated cells identified by Pacific Blue fluorescence.

Transient transfections and sorting. MDCK stably expressing clones were transiently transfected using Lipofectamine 2000 (Invitrogen) according to the manufacturer's directions, using 3 to 12 μg total DNA, depending on the experiment. All the transfections were performed using a construct expressing green fluorescent protein (pEGFP-N1; Clontech) as a marker for cell sorting in combination with either wild-type p70S6K (wt-p70S6K), constitutively active MEK (CA-MEK), or eIF4E constructs. The following day, cells were analyzed with a FACS Vantage DIVA sorter (Becton Dickinson). GFP-positive cells were sorted and replated in 60-mm dishes. After 36 h, half were analyzed by Western blotting and the second half were reanalyzed by FACS to determine the cell cycle and cell size as described above. The cells used for the Western blot analysis were harvested after an overnight starvation period. Each experiment was performed a minimum of three times.

For targeted silencing, SiGENOME ON-TARGETplus SMARTpool directed against murine eIF4E (catalog no. L-040708-00-0010), murine p70S6K (L-040893-00-0010), murine ERK1 or -2 (L-040613-00-0010, L-040126-00-001), and a control non-targeting murine pool (D-001810-10-0020) were purchased from DHARMACON Inc. and transiently transfected into cells using Lipofectamine for 48 h, following the manufacturer's instructions.

Generation of a conditional mouse line (*Pkd1*$^{flox/flox}$) and isolation of mouse embryonic fibroblasts (MEFs). The full description of the *Pkd1*^{flox} mice will be provided elsewhere (C. Wodarczyk and A. Boletta, unpublished data). In brief, a targeting vector carrying the genomic region between *Pkd1* exon 39 and Tsc2 exon 30 was generated. LoxP sites were inserted into intron 43 and into the 3′ untranslated region of the *Pkd1* gene. The neomycin cassette for selection of embryonic stem clones, flanked by Frt sites, was inserted into the *Pkd1*/*Tsc2* 63-bp inter-region. Correctly targeted embryonic stem cells were identified by PCR/Southern blotting and subsequently injected into blastocysts to generate chimeric animals and finally *Pkd1*$^{flox/+}$ mice. The Neo cassette was removed by crossing the mice with a Flp-expressing line. The resulting heterozygous *Pkd1*$^{flox/+}$ mice were intercrossed to generate *Pkd1*$^{flox/flox}$ mouse lines. Inactivation using a ubiquitous Cre recombinase resulted in embryonic lethality and a phenotype very similar to that of null mice.

Primary MEF cells were isolated from either E11.5 C57BL/6 *Pkd1*$^{flox/flox}$ or *Pkd1*$^{-/-}$ embryos (in which exons 2 to 3 of murine *Pkd1* were replaced with the *lacZ* gene cloned in frame to the 5′ end of exon 2 of *Pkd1* [2]) from two litters of heterozygous crosses. Whole embryos (excluding the heads) were mechanically dissociated, washed, trypsinized for 15 min, and cultured in six-well tissue culture plates. Cells were maintained in Dulbecco's minimal essential medium containing 10% fetal bovine serum. Genotyping was carried out by PCR on the heads of the embryos. Five sets of MEFs were isolated: the no. 11 and 14 MEFs (from *Pkd1*$^{+/+}$ and *Pkd1*$^{-/-}$ mice) were used for analysis both as primary cultures (data not shown) and as immortalized MEFs. Two additional sets (no. 16 and 19 and no. 35 and 38 from *Pkd1*$^{+/+}$ and *Pkd1*$^{-/-}$) were only employed as primary cultures. Two sets (Flox1 and Flox2) were isolated from *Pkd1*$^{flox/flox}$ mice and immortalized. Primary MEFs were used up to passage 8. MEFs were spontaneously immortalized following the NIH 3T3 method, by continuous passaging at a 1:3 dilution three times a week.

For conditional inactivation of the *Pkd1*$^{flox/flox}$ lines, cells were incubated in the presence of a recombinant TATCre protein, allowing for the efficient inactivation of the gene in the absence of any integration within the genome, which

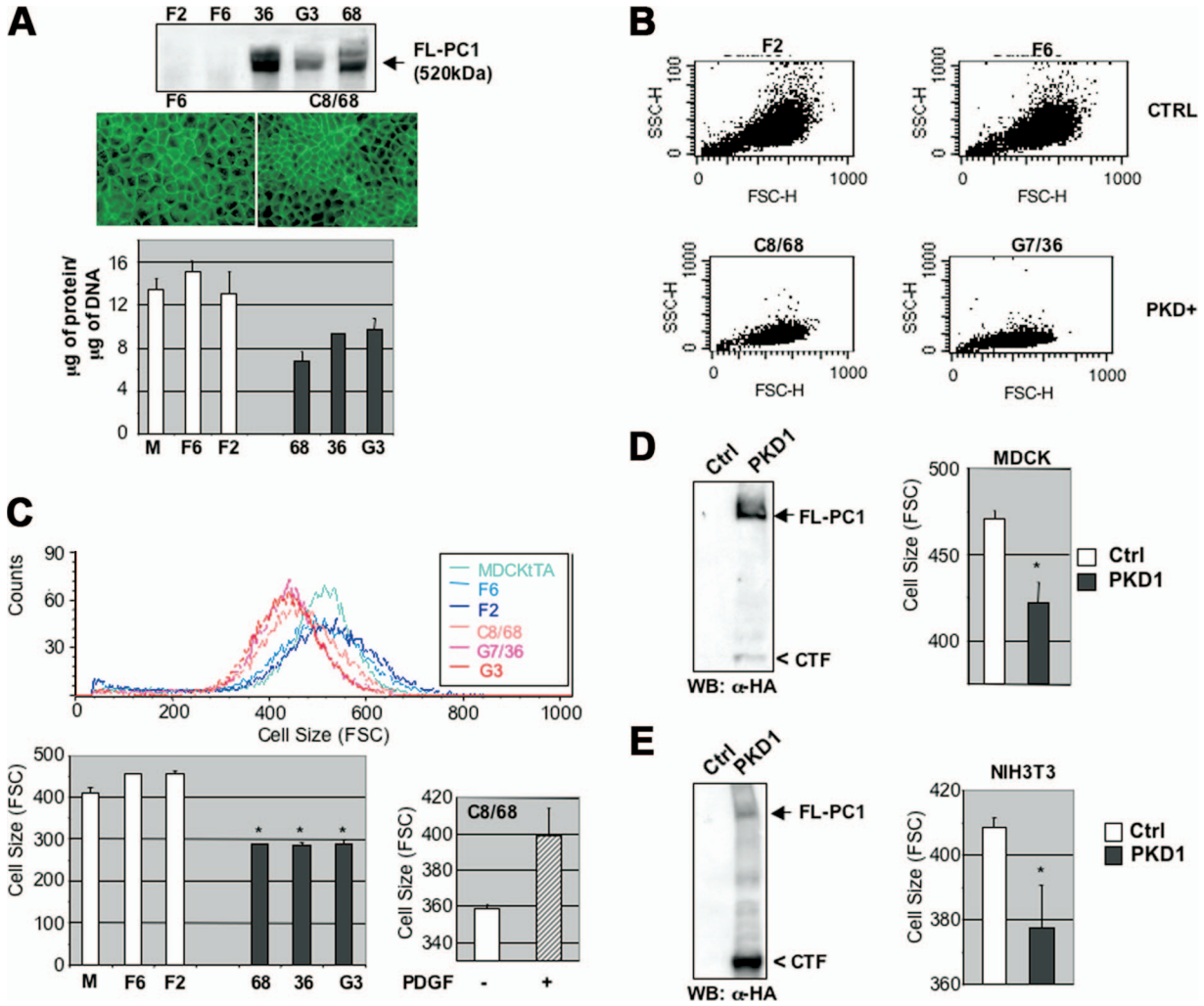

FIG. 1. PC-1 overexpression induces reduced cell growth and size in MDCK cells. (A) (Top) Two MDCK Zeo controls (F6 and F2) and three independently derived MDCK *PKD1* Zeo cell lines (G7/36 [36], C8/68 [68], and G3) were subject to Western blot analysis using an anti-PC-1 antibody. (Middle) Confluent monolayers of control MDCK Zeo (F6) and MDCK *PKD1* Zeo cells (C8/68) were stained with an anti-E-cadherin antibody (green). The microphotographs were taken at equal magnifications (×40). (Bottom) The total content in μg of protein per μg of DNA was determined in three independently derived MDCK *PKD1* Zeo cells (C8/68 [68], G7/36 [36], and G3) and three control cell lines (MDCKtTA [M], F6, and F2). (B) The same cell lines as in panel A were trypsinized and analyzed using a flow cytometer (FACS). Each spot represents a single cell, and the FSC-H values on the *x* axis represent the size measurements of the cells. SSC-H, side scattered light height (C) The same cell lines as in panel A were analyzed as in panel B and plotted on a single plot for comparison (red lines, MDCK *PKD1* Zeo; blue lines, controls). (Bottom left) Histogram representation of the average FSC values of the six clones shown in the top plot, repeated in triplicate. Statistical analysis was performed by applying ANOVA (*, $P < 0.0001$). (Bottom right) Histogram representation of cell size after treatment with PDGF. (D) (Left) Western blot analysis of total lysates of MDCK cells transiently transfected with GFP alone (Ctrl) or in combination with a HA-*PKD1* construct reveals the presence of both the full-length protein (arrow) and the C-terminal fragment (CTF) cleaved form (arrowhead). (Right) Quantification of the cell size (FSC-H) of transiently transfected MDCK cells was performed as described for panel B. Statistical analysis was performed by applying the Student's *t* test (*, $P < 0.05$). (E) The identical experiment as in panel D was repeated on NIH 3T3 cells. Statistical analysis was performed by applying the Student's *t* test (*, $P < 0.05$).

could potentially cause clonality effects (as previously described in reference 19). For genotyping the *Pkd1*$^{flox/flox}$ MEFs before and after excision with the Cre, the following primers were used: the forward primer Tag5 (CAC AAT GGA CCT CCT TCC TC), which binds in *Pkd1* exon 46, and the reverse primer Tag3 (TCT GAG AGG CCA GTG TGA AG), which targets the 3′ untranslated region of *Pkd1*. A third forward primer, 43MR (TGC TGC TGT TTG CCC TAT AC), binds in *Pkd1* exon 43 and was included in the PCR. Before excision, only the Tag5 and Tag3 primers would amplify a signal because the 43MR and Tag3 primers were too distant. After excision, this second set of primers became active and amplified a larger band.

Cell size, cell cycle, and Western blot analyses were carried out on primary, immortalized, and conditionally inactivated MEFs and generated similar results.

Statistical analysis. Statistical analysis was performed by applying either a Student's *t* test (Fig. 1D, 1E, 2D, 3E, 4C, 4D, 5C bottom, and 7D) or one-way analysis of variance (ANOVA) (Fig. 1C, 3A, 3D, 4A, 4B, 5C top, 6C, 7B, 7C, 8A, and 8C). Multiple comparisons were carried out using Fisher's PLSD parameters. The different *P* values obtained are indicated in the legends of the figures.

RESULTS

PC-1 regulates cell size in a cell cycle-independent manner. We have previously described a set of MDCK cells overexpressing full-length human PC-1 (Fig. 1A, top panel) (5).

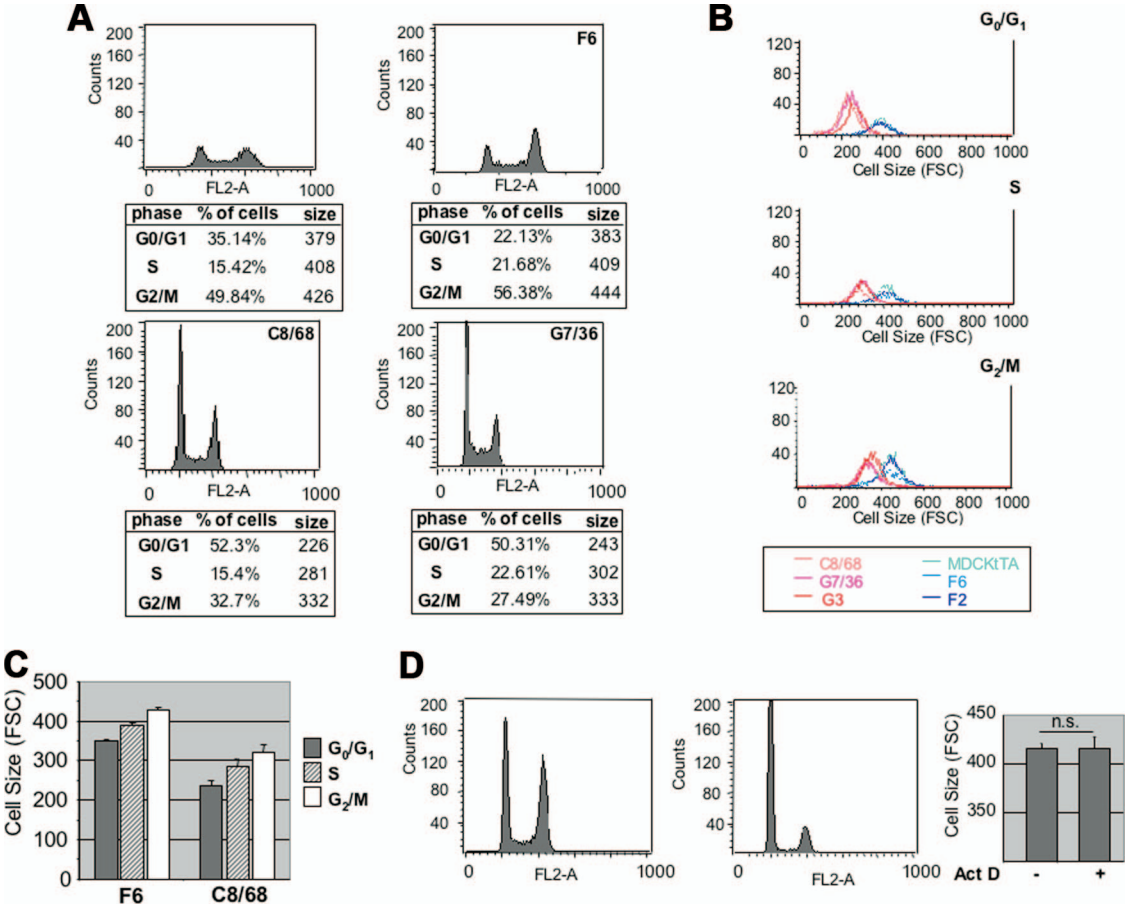

FIG. 2. PC-1 regulation of cell size is cell cycle independent. (A) Cells were plated at 50% confluence and serum starved. After 24 h, they were fixed and stained using PI to determine their DNA content (on the *x* axis is fluorescence intensity). Cell size profiles were analyzed in each of the three phases of the cell cycle. The tables below the graphs show the percentages of cells in the G_0/G_1, S, and G_2/M phases of the cell cycle and their mean FSC-H values, reflecting cell size (right column). (B) Single-plot representation of the distribution of sizes of cells in each of the three phases of the cell cycle. The difference in the FSC values was maintained in each phase, with much lower values in MDCK *PKD1* Zeo clones (C8/68, G7/36, and G3) than in the negative controls (MDCKtTA, F6, and F2). (C) Histogram representation of the distribution of cell size in each phase of the cell cycle shows an increase in cell size. (D) $Pkd1^{+/+}$ (no. 11 and 16) and $Pkd1^{-/-}$ (no. 14 and 19) cells were treated as described for panel A, and cell size profiles were analyzed in the G_0/G_1 phase of the cell cycle. (Right) MDCK cells were treated overnight with vehicle only (left bar) or with 15 μM of actinomycin D (right bar; ActD). Upon treatment, cells are arrested in the G_0/G_1 phase of the cell cycle. Quantification of the cell size for cells in G_0/G_1 revealed no differences in size between untreated cells and those treated with actinomycin D. Statistical analysis was performed by applying the Student's *t* test. n.s., not statistically significant.

While culturing these cell lines, we noticed that three independently derived MDCK *PKD1* Zeo clones (C8/68) appeared smaller than their counterpart MDCK Zeo controls (F6) (Fig. 1A, middle panel). In addition, their protein content per DNA content was significantly reduced (Fig. 1A, bottom graph).

To quantify and further validate this observation, we analyzed MDCK Zeo controls and MDCK *PKD1* Zeo cells by testing their forward laser light scatter (FSC-H) using a flow cytometer. As shown in Fig. 1B, MDCK *PKD1* Zeo (C8/68 and G7/36) cells are smaller (FSC on the *x* axis) than the controls (F6 and F2). Comparing the sizes of three control cell lines (MDCKtTA, F6, and F2) and three independently derived MDCK *PKD1* Zeo clones (C8/68, G7/36, and G3) revealed that the latter are considerably smaller (Fig. 1C, red lines versus blue lines), with the mean FSC values for PC-1-overexpressing cells (C8/68, 287 ± 1; G7/36, 286 ± 6; G3, 289 ± 9) being significantly lower than those of the controls (MDCKtTA, 411 ± 11; F6, 455 ± 1; F2, 457 ± 6 [$P < 0.0001$]) (Fig. 1C, bottom). To formally exclude the possibility of clonal effects, we transiently transfected PC-1 into MDCK and NIH 3T3 cells and found that, in both cell types, the overexpression of PC-1 leads to a statistically significant reduction in cell size (Fig. 1D and E). We therefore conclude that PC-1 reduces the sizes of cells both in renal epithelial cells (MDCK) and in fibroblasts (NIH 3T3).

PC-1 regulation of cell size is not secondary to cell cycle regulation. It is widely reported that cells dividing symmetrically increase in size during the progression of the cell cycle from the G_0/G_1 to the S and G_2/M phases (8, 9). Since we and other groups have previously reported that PC-1 induces cell cycle arrest in the G_0/G_1 phase of the cell cycle (2, 5, 22), we wondered if the reduced average size of cells expressing *PKD1* simply reflected a higher proportion of cells in G_0/G_1 (Fig. 2A). As shown in Fig. 2, PC-1-overexpressing cells (red lines)

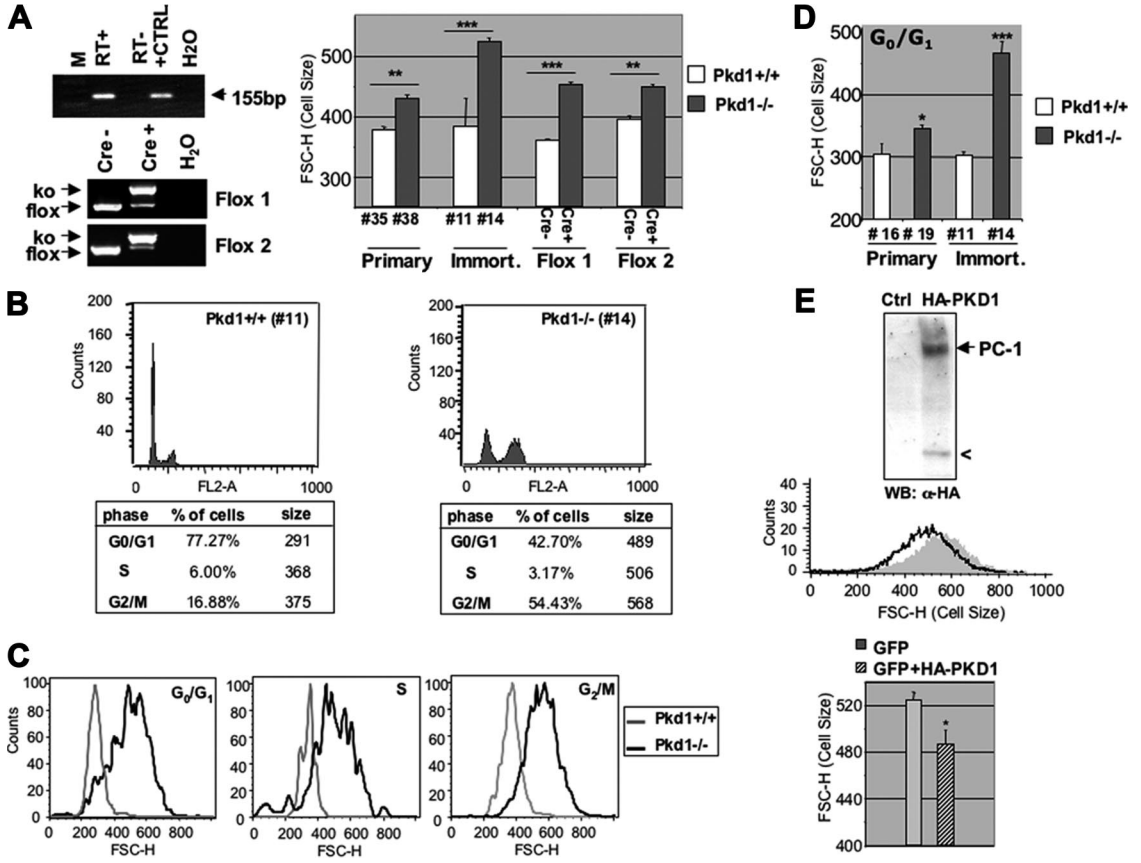

FIG. 3. Cell cycle-independent increase in cell size in *Pkd1*$^{-/-}$ MEFs. (A) (Top left) RT-PCR performed on RNA isolated from wt MEFs isolated at day E11.5. Total RNA incubated in the presence (RT+) or absence (RT−) of retrotranscriptase and subjected to PCR analysis revealed that the *Pkd1* gene is expressed in these cells. (Bottom left) PCR analysis of the MEFs derived from a conditional mouse model (*Pkd1*$^{flox/flox}$) treated in the presence (Cre+) or absence (Cre−) of a Cre recombinase (see Materials and Methods) shows that the last two exons have been successfully excised (ko) at a high rate. (Right) Statistical analysis of the differences in cell sizes between *Pkd1*$^{+/+}$ and *Pkd1*$^{-/-}$ MEFs either isolated as primary culture (no. 35 and 38) or immortalized (no. 11 and 14), as well as two independently derived MEFs generated from a conditional mouse model (*Pkd1*$^{flox/flox}$) and treated in the presence (Cre+) or absence (Cre−) of Cre recombinase, revealed that, independently of the method employed, the absence of the *Pkd1* gene always results in cells significantly larger than their counterpart controls. Statistical analysis was performed by applying ANOVA (**, $P < 0.005$; ***, $P < 0.0001$). The minor differences in size observed among the different *Pkd1*$^{+/+}$ MEFs were not statistically significant. (B) Cells were plated at 50% confluence and serum starved, and after 24 h, they were fixed and stained using PI as described for Fig. 2. Top graphs show the analysis of the cell cycle, revealing that *Pkd1*$^{-/-}$ has a higher proportion of cells in the G_2/M phase of the cell cycle than do *Pkd1*$^{+/+}$ MEFs. The tables below the graphs show the percentages of cells in G_0/G_1, S, and G_2/M phases of the cell cycle and their mean FSC-H values (sizes, right column). The cell size profiles analyzed in each phase of the cell cycle revealed that the *Pkd1*$^{-/-}$ cells are larger in size, independent of their cell cycle state. (C) Single plot representation of the distribution of cell sizes of the *Pkd1*$^{+/+}$ (no. 11, light lines) and *Pkd1*$^{-/-}$ (no. 14, dark lines) MEFs in each phase of the cell cycle, as analyzed in panel B. (D) *Pkd1*$^{-/-}$ MEFs are larger in size, independent of the cell cycle phase in which they are analyzed. Statistical analysis was performed by applying ANOVA (*, $P < 0.05$; ***, $P < 0.0001$). (E) Transient transfection of full-length PC-1 into *Pkd1*$^{-/-}$ MEFs (top Western blot) leads to a reduction in the distribution of cell size (middle plot) that is statistically significant (bottom histograms). Statistical analysis was performed by applying the Student's *t* test (*, $P < 0.01$).

are smaller than the controls (blue lines) in each of the three phases analyzed (G_0/G_1, S, and G_2/M; Fig. 1A and B), although their size increases during cell cycle progression at a slightly higher rate than the controls (Fig. 2A, bottom tables, and C). Finally, we artificially arrested MDCK cells in G_0/G_1 using actinomycin D (Fig. 2D), and we compared the sizes of the cells in G_0/G_1 before and after inducing cell cycle arrest. We found that the arrest of cells in G_0/G_1 is not sufficient per se to induce a reduction in cell size (Fig. 2D, right panel). These data demonstrate that PC-1 controls both cell proliferation and cell growth in MDCK cells and that the latter is not merely a result of the former.

Cell cycle-independent increase in cell size in *Pkd1*$^{-/-}$ MEFs. We next searched for a cell system in which we could test if the absence of PC-1 would result in an opposite effect, i.e., increased cell size. We thus isolated MEFs from wt mice and tested if the *Pkd1* gene is expressed. Reverse transcriptase (RT)-PCR analysis revealed that MEFs isolated at embryonic day 11.5 (E11.5), as well as at different embryonic days, do express the *Pkd1* gene (Fig. 3A; also data not shown). We therefore isolated MEFs from E11.5 *Pkd1*$^{+/+}$ and *Pkd1*$^{-/-}$ littermates (see Materials and Methods) (2). The morphology of the MEF cell lines visualized by light microscopy seemed to suggest an enlarged phenotype of the *Pkd1*$^{-/-}$ cells compared

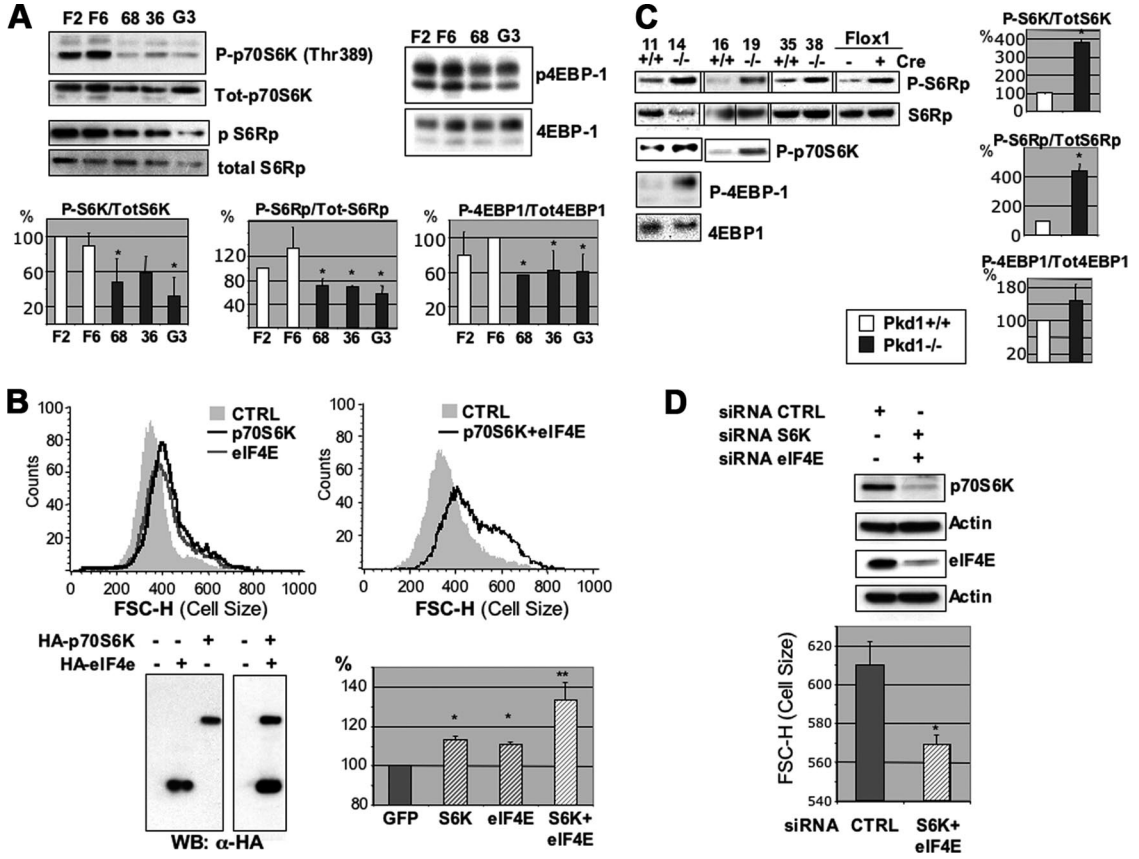

FIG. 4. PC-1 effects on cell growth and size are mediated by the mTOR/p70S6K pathway. (A) In total, two different MDCK Zeo (F2 and F6) and three different MDCK *PKD1* Zeo (C8/68 [68], G7/36 [36], and G3) cells were plated at 50% density in 0.5% FCS. After 12 h, total lysates were analyzed using anti-phospho-Thr389-p70S6K, anti-phospho-S6Rp, or anti-4EBP1 protein. Blots were stripped and reprobed with antibodies against p70S6K, S6Rp, or tubulin, revealing the total amounts loaded in each lane. Quantification of the blots showed reduced phosphorylation of p70S6K, S6Rp, and 4EBP1 in MDCK *PKD1* Zeo cells compared to the levels in controls (bottom histograms). Statistical analysis was performed by applying ANOVA (*, $P < 0.05$). (B) The C8/68 MDCK *PKD1* Zeo cell line was transiently transfected with GFP along with either p70S6K alone (dark line), eIF4E alone (light line), or p70S6K and eIF4E in combination (dark line in the right-hand plot). The last condition completely restores cell size over the control GFP-transfected cells, while transfection of the single molecules alone had a smaller, though significant, effect. Statistical analysis was performed by applying ANOVA (*, $P < 0.05$; **, $P < 0.0001$). (C) The identical experiment as shown in panel A was performed on $Pkd1^{+/+}$ (no. 11, 16, and 35) and $Pkd1^{-/-}$ (no. 14, 19, and 38) MEFs as well as on Pkd Flox-1 MEFs, revealing increased phosphorylation of p70S6K, S6Rp, and 4EBP1 in $Pkd1^{-/-}$ cells compared to the levels in $Pkd1^{+/+}$ (right-hand histograms). Statistical analysis was performed by applying the Student's *t* test (*, $P < 0.05$). (D) The $Pkd1^{-/-}$ MEFs (no. 14) were transiently transfected either with control siRNAs or with siRNAs directed against murine p70S6K and eIF4E. Combined silencing of the two molecules is able to reduce the cell size in these MEFs. Statistical analysis was performed by applying the Student's *t* test (*, $P < 0.05$).

to the size of the wt cells (data not shown). In Fig. 3A, we show a quantification using FACS analysis. Two independently derived $Pkd1^{-/-}$ MEFs (no. 14 and 38) showed a significant increase in their overall cell size compared to that of control wt MEFs (no. 11 and 35). This was independent of whether the MEFs were primary cultures (no. 35 and 38; also data not shown) or immortalized cell lines (no. 11 and 14). Since the differences observed in these cell lines might be attributed to a clone-to-clone variation effect, to exclude this possibility we isolated MEFs from a mouse model carrying Floxable alleles of the *Pkd1* gene (Wodarczyk and Boletta, unpublished) (also see Materials and Methods). Two independent MEF lines ($Pkd1^{flox/flox}$) were isolated and immortalized (Flox1 and Flox2). To achieve inactivation of the *Pkd1* alleles without introducing clonal effects due to genomic integration of the Cre gene, we used a cell-permeable TATCre fusion protein capable of efficiently inducing the recombination of *loxP* sites and that is subsequently degraded by the cells (19) (also see Materials and Methods). Treatment with the Cre recombinase resulted in a minimum of 70 to 80% inactivation of the *Pkd1* allele, as assessed by PCR analysis of the genomic DNA (Fig. 3A, bottom left). Quantification of the cell size showed a statistically significant difference between the sizes of MEFs before and after inactivation of the *Pkd1* gene (Fig. 3A, bottom left). These data demonstrate that the absence of the *Pkd1* gene results in increased cell size independently of the MEF line isolated.

Next, we analyzed the cell cycle profile of the knockout cell lines and found that the $Pkd1^{-/-}$ MEFs have an altered cell cycle profile compared to that of the wt $Pkd1^{+/+}$ cells (Fig. 3B, bottom tables) but, again, the cell size is increased in each of the cell cycle phases analyzed in several MEF lines tested (Fig. 3B, bottom tables, and C and D; also data not shown). Finally, in order to exclude the possibility that the procedures of isolation or immortalization, rather than the absence of the *Pkd1*

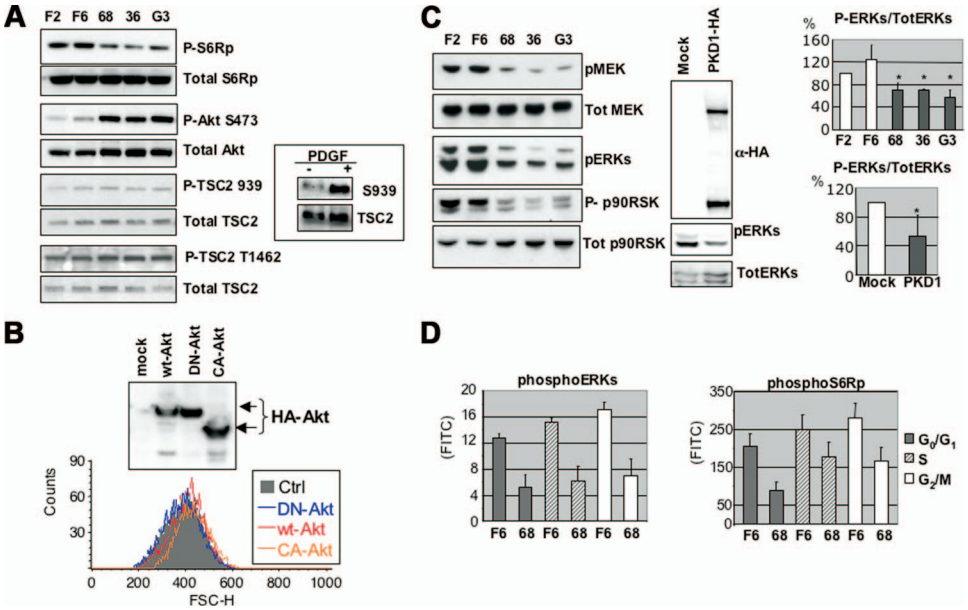

FIG. 5. PC-1 controls cell size in an Akt-independent manner and is able to downregulate the ERKs. (A) Control cell lines (F6 and F2) and MDCK *PKD1* Zeo clones (C8/68 [68], G7/36 [36], and G3) were plated at 50% confluence in 0.5% serum for 12 h. Western blot analysis was carried out using anti-P-S6Rp, anti-P-Ser473-Akt, anti-P-Thr1462, and anti-P-Ser939-tuberin antibodies. Each blot was stripped and reprobed using antibodies against the total corresponding protein. (Inset blot) Anti-P-Ser939 antibodies are able to detect an increase in phosphorylation of tuberin in NIH 3T3 cells treated in the presence of PDGF (+) compared to those treated in the absence of PDGF (−), demonstrating the good quality of the antibodies. (B) Overexpression of wt-, DN-, or CA-Akt in the C8/68 clone revealed that DN-Akt is not able to regulate cell size, while both wt-Akt and CA-Akt are able to induce an increase in cell size, despite the equal transfection levels of all three constructs (top Western blot). (C) (Left) Control cell lines (F6 and F2) and MDCK *PKD1* Zeo clones (C8/68 [68], G7/36 [36], and G3) were probed using antibodies against phosphorylated forms of MEK, ERK, and p90RSK, showing a dramatic downregulation of the ERK pathway. Blots were stripped and probed using anti-total MEK or anti-total p90RSK and revealed that no differences in loading could account for this downregulation. (Middle) Transient transfection of full-length *PKD1*-HA in NIH 3T3 cells, followed by Western blotting with anti-HA and anti-phospho-ERK antibodies. Transfection of PC-1 results in downregulation of phospho-ERKs. The blot was stripped and probed with total ERKs. (Right) Quantification of the phosphorylation levels of ERKs in stable MDCK transfectants (top) or in transiently transfected NIH 3T3 cells (bottom). Statistical analysis was performed by applying either ANOVA (top) or the Student's *t* test (bottom) (*, $P < 0.05$). (D) Cells were trypsinized, fixed, and double-stained for DNA content (DAPI) and with anti-phospho-ERK (left graph) or anti-phospho-S6Rp (right graph) antibodies. The content of phosphorylated molecules per single cell was evaluated in each phase of the cell cycle (see Materials and Methods).

gene, were responsible for the changes in cell size, we reexpressed wt *PKD1* in knockout MEFs (no. 14) and we found that PC-1 significantly reduced the size of these cells (Fig. 3E). We therefore conclude that the absence of the *Pkd1* gene correlates with increased proliferation and cell size in MEFs and that there is a direct correlation between the presence or absence of PC-1 and cell size.

The PC-1 effects on size are mediated by the mTOR pathway and its downstream effectors p70S6K and 4EBP1. One of the cascades controlling cell growth and size is the mTOR pathway, leading to the phosphorylation of both p70S6K and 4EBP1 (31). Using phosphor-specific antibodies, we analyzed the phosphorylation status of this cascade and found that p70S6KThr389, S6Rp, and 4EBP1 phosphorylation levels were reduced in MDCK *PKD1* Zeo cells compared to the levels in controls (Fig. 4A). Stripping and reprobing the same membranes with anti-p70S6K, anti-S6Rp, or anti-4EBP1 antibodies revealed that differences in loading could not account for such a downregulation (Fig. 4A). To determine if reestablishing high levels of activity of these two molecules would be sufficient to revert the PC-1 effects on cell size, we transiently transfected p70S6K and eIF4E independently or in combination in MDCK *PKD1* Zeo cells, along with GFP, and analyzed their cell size profiles after 24 h. As shown in Fig. 4B, both molecules are separately able to increase the cell size of the C8/68 cell line and, when both molecules are transfected in combination, the cell size is increased to a much greater extent, suggesting that the two branches of the cascade are cooperating in regulating cell size. The cell cycle profile of the MDCK *PKD1* Zeo cells expressing p70S6K was also affected, with an increased number of cells in the G_2/M phase compared to the number in GFP-transfected cells (data not shown). However, the size of the cells was increased in each cell cycle phase, excluding the increased number of cells in G_2/M as the trivial explanation for our findings (data not shown).

Finally, we tested whether the same pathway is upregulated in *Pkd1*$^{-/-}$ MEFs. The analysis of the phosphorylation levels of p70S6K, S6Rp, and 4EBP1 in lysates derived from *Pkd1*$^{-/-}$ MEFs (no. 14 and 19) revealed a marked increase compared to the levels in *Pkd1*$^{+/+}$ controls (no. 11 and 16) (Fig. 4C). Silencing either p70S6K or eIF4E had a mild effect on restoring the cell size in *Pkd1*$^{-/-}$ MEFs (data not shown), while cosilencing both molecules resulted in a significant reduction in cell size (Fig. 4D). We conclude that both the p70S6K/S6Rp and 4EBP1/eIF4E complexes are involved in regulating cell size in response to PC-1.

PC-1 controls cell size and the mTOR pathway in an Akt-independent, ERK-dependent manner. The apparent decrease in mTOR kinase activity in response to PC-1 overexpression is somewhat surprising, because our previous studies demonstrated that PC-1 induces activation of the serine/threonine kinase Akt (3, 4), one of the major activators of the Tsc2/mTOR pathway. We therefore investigated the potential role of Akt in our system. Surprisingly, despite the profound inhibition of S6Rp phosphorylation in three independent MDCK *PKD1* Zeo cell lines, Akt is strongly phosphorylated in the same lysates, suggesting a disconnect between Akt activation and mTOR regulation in our cellular system (Fig. 5A). Consistent with this, using epitope-specific anti-Tsc2 antibodies directed against the Akt phospho-specific sites Thr1462 or Ser939 (25), we found no changes in the MDCK *PKD1* Zeo cells compared to controls. Probing with the same antibodies, lysates derived from NIH 3T3 cells treated with platelet-derived growth factor (PDGF) revealed an increase in the phosphorylation of Tsc2 in the Akt phospho-specific sites, showing the functionality of the antibodies (Fig. 5A). In order to further investigate the role of Akt in our system, we expressed a set of Akt constructs, including wt-Akt, a dominant negative form (DN-Akt), and CA-Akt, along with GFP in MDCK *PKD1* Zeo cells, and analyzed the effect on cell size as a readout of the mTOR pathway. We failed to observe an effect on cell size upon expression of a DN-Akt construct in these cells (Fig. 5B), consistent with the disconnection between Akt activation and mTOR regulation observed in Fig. 5A. However, the expression of the same construct reversed the anti-apoptotic effects of PC-1 in these same cells (3; also data not shown), demonstrating its functionality. Interestingly, we also observed that both wt-Akt and, to a greater extent, CA-Akt are able to increase cell size in the controls and to restore normal cell size in MDCK *PKD1* Zeo cells. This suggests that, as shown in Fig. 5A, when Akt is activated through a different system, it is indeed able to act on the mTOR pathway in this cell type.

Recent reports have demonstrated that the ERKs p42/p44 control the mTOR pathway by directly phosphorylating Tsc2 and releasing the inhibitory activity of the tuberin/hamartin complex (23, 24). We therefore investigated the status of the activation of the ERK pathway in our system and found that p90RSK, the p42/p44 ERKs, and MEK kinases are strongly downregulated in MDCK *PKD1* Zeo cells compared to the levels in the controls (Fig. 5C). Furthermore, transient expression of full-length PC-1 in NIH 3T3 cells led to the downregulation of the ERKs (Fig. 5C), demonstrating that clonal artifacts cannot account for the effect observed in the MDCK cells. Analysis by flow cytometry revealed a marked difference between control (F6) and MDCK *PKD1* Zeo cells (C8/68) in the activation statuses of both S6Rp and the ERKs in each phase of the cell cycle. Furthermore, the two molecules seem to be similarly regulated during progression through the cell cycle (Fig. 5D).

Taken together, these data demonstrate that the overexpression of PC-1 leads to the downregulation of the ERKs both in epithelial cells (MDCK) and fibroblasts (NIH 3T3) and that this correlates with a downregulation in the mTOR pathway.

To test if the changes in ERKs are responsible for the regulation of the mTOR pathway and cell size by PC-1, we transiently transfected MDCK *PKD1* Zeo cells with a dominant positive construct of MEK kinase (CA-MEK), cotransfected with GFP, and analyzed the cell cycle and cell size profiles after sorting. We found that CA-MEK restored the phosphorylation levels of pS6Rp and the cell size of the MDCK *PKD1* Zeo clone C8/68 (Fig. 6A). Since the ERKs can directly act on S6K/S6Rp without acting through mTOR, we questioned whether this effect occurs dependently or independently of the mTOR pathway. We show in Fig. 6B that the inhibition of mTOR using rapamycin completely blocked the CA-MEK effect on S6Rp phosphorylation and cell size, demonstrating that mTOR is required for this effect (Fig. 6B). Consistent with this, the transient transfection of

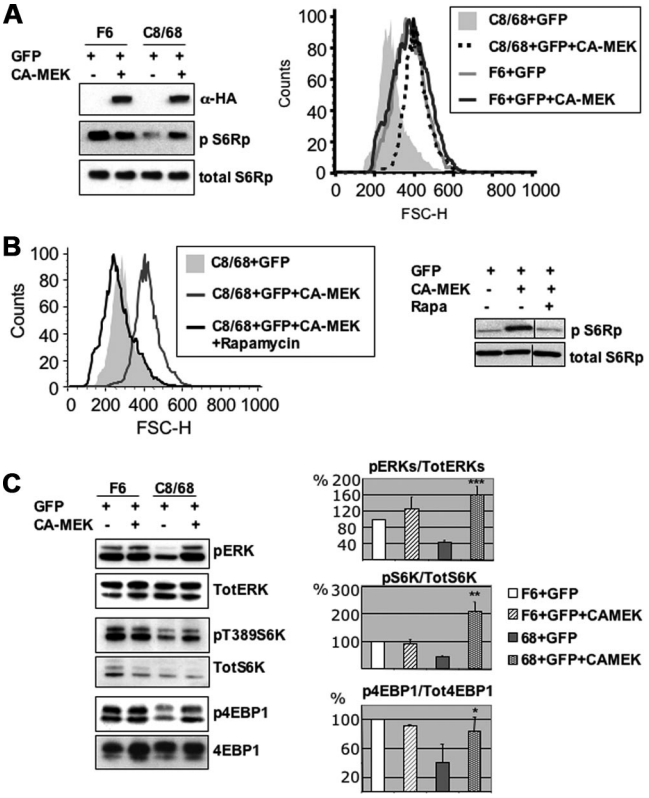

FIG. 6. CA-MEK reverts PC-1 control of cell size and mTOR. (A) A total of 12 μg of a construct encoding the catalytically active form of MEK (CA-MEK) was transiently transfected in control (F6) and MDCK *PKD1* Zeo (C8/68) cells along with GFP, and then the cells were sorted and replated. Cells were analyzed for their cell size profiles 24 h after replating. CA-MEK was able to increase both the phosphorylation levels of S6Rp and the cell size. Anti-HA antibodies revealed that comparable expression levels were achieved in both controls and MDCK *PKD1* Zeo cells. (B) Transient transfection of GFP alone or in combination with CA-MEK was carried out as described for panel A in the C8/68 cell line. Cells were treated in the presence or absence of rapamycin and subjected to Western blot analysis using antibodies against phospho-S6Rp or to FACS analysis to determine their FSC values, reflecting cell size. Treatment in the presence of rapamycin prevents the recovery of phospho-S6Rp (right) and cell size (left) induced by CA-MEK, demonstrating that CA-MEK acts through mTOR to exert its function. (C) GFP-positive cells transiently transfected as described for panel A were sorted, replated, serum starved overnight, and analyzed biochemically using the antibodies indicated. Transfection of CA-MEK in *PKD1*-overexpressing cells restores phosphorylation of both p70S6K and 4EBP1. Histograms on the right show the averages of quantifications of Western blots from at least three different experiments. Statistical analysis was performed by applying ANOVA (*, $P < 0.05$; **, $P < 0.005$; ***, $P < 0.0001$).

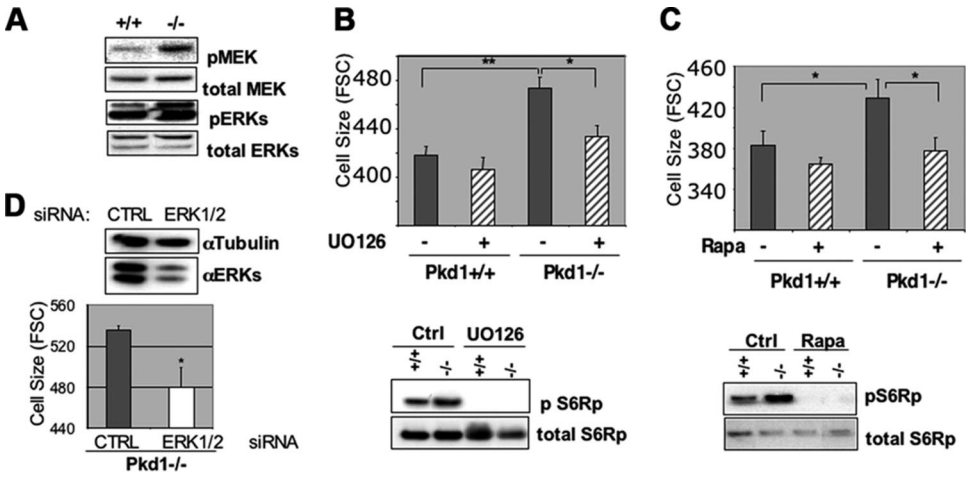

FIG. 7. Impaired ERK and mTOR activities are responsible for increased cell size in *Pkd1*$^{-/-}$ MEFs. (A) Western blot analysis of total lysates from *Pkd1*$^{+/+}$ and *Pkd1*$^{-/-}$ MEFs using anti-phospho-specific antibodies for MEK and ERKs revealed that the phosphorylation levels of these molecules are increased in *Pkd1*$^{-/-}$ MEFs compared to the wt levels. Stripping and reprobing the same membrane using antibodies directed against the total levels of the same molecules revealed that all lanes were loaded equally. (B) (Top) *Pkd1*$^{+/+}$ and *Pkd1*$^{-/-}$ MEFs were treated in the presence or absence of the MEK inhibitor U0126. Statistical analysis was performed by applying ANOVA (*, $P < 0.05$; **, $P < 0.005$). (Bottom) Western blot analysis of the same samples shown on top revealed that treatment in the presence of U0126 diminishes the phosphorylation levels of S6Rp. (C) Identical experiment as described for panel B, except that cells were treated in the presence or absence of rapamycin to inhibit mTOR activity. Statistical analysis was performed by applying ANOVA (*, $P < 0.05$). (D) Transient transfection of siRNAs directed against murine ERK1 and -2 into *Pkd1*$^{-/-}$ cells results in a significant reduction of the expression levels of the ERKs and, concomitantly, a significant reduction of cell size. Statistical analysis was performed by applying the Student's *t* test (*, $P < 0.05$).

CA-MEK restored the phosphorylation levels of Thr389 in p70S6K, as well as the phosphorylation of 4EBP1, both of which are downstream targets of mTOR kinase activity (Fig. 6C). We conclude that MEK acts through the regulation of mTOR to rescue the cell size phenotype.

Next, we tested for the phosphorylation levels of the MEK/ERK pathway in the MEF cells and found that this cascade is strongly upregulated in *Pkd1*$^{-/-}$ cells compared to the level in *Pkd1*$^{+/+}$ MEFs (Fig. 7A). Furthermore, the inhibition of mTOR (using rapamycin; Fig. 7C) or MEK (using U0126; Fig. 7B) or the silencing of ERKs using small interfering RNA (siRNA) (Fig. 7D) were all able to revert the cell size phenotype as well as the increased phosphorylation levels of S6Rp in *Pkd1*$^{-/-}$ MEFs (Fig. 7B and C).

We therefore conclude that the regulation of the ERK pathway is the primary mechanism through which PC-1 regulates the mTOR cascade, its downstream targets p70S6K and 4EBP1, and cell growth (size).

PC-1-dependent regulation of cell size and the mTOR pathway is mediated by the ERK-dependent regulation of tuberin. To further investigate the role of tuberin in the PC-1-induced reduction of cell size, we expressed full-length PC-1 in *Tsc2*$^{+/+}$; p53$^{-/-}$ and *Tsc2*$^{-/-}$; p53$^{-/-}$ MEFs, synchronized the cells in the G_0/G_1 phase of the cell cycle, and analyzed the cell size profiles. We found that PC-1 is able to reduce cell size in a statistically significant manner only in MEFs expressing tuberin (*Tsc2*$^{+/+}$; p53$^{-/-}$) and not in MEFs lacking it (*Tsc2*$^{-/-}$; p53$^{-/-}$), despite the fact that equal expression levels of PC-1 are achieved in both cell lines (Fig. 8A). These data suggest that the PC-1 effect on cell size requires tuberin. To directly test whether ERK-dependent regulation of tuberin stands as the basis of our observations, we checked the status of S664 phosphorylation of tuberin (one of the ERK-specific phosphosites) using a novel antibody generated to specifically recognize this phosphorylation site (23). We show in Fig. 8B that the phosphorylation levels of tuberin at S664 are reduced in three independent MDCK *PKD1* Zeo clones (C8/68, G7/36, and G3) compared to the levels in controls (F6 and F2). Conversely, the phosphorylation levels of tuberin in S664 in the *Pkd1*$^{-/-}$ MEFs are increased compared to the levels in *Pkd1*$^{+/+}$ controls.

Finally, in order to make sure that the differential effects on cell size observed by the expression of PC-1 in *Tsc2*$^{+/+}$; p53$^{-/-}$ or *Tsc2*$^{-/-}$; p53$^{-/-}$ cells are directly due to the absence or presence of tuberin and not to differences in the isolation or immortalization process of these fibroblasts, we restored the expression of wt Tsc2 in the *Tsc2*$^{-/-}$; p53$^{-/-}$ MEFs alone or in combination with PC-1. We show in Fig. 8C that wt tuberin reduces the cell size in *Tsc2*$^{-/-}$; p53$^{-/-}$ MEFs and that the coexpression of full-length PC-1 is able to further enhance this effect, in a statistically significant manner. A mutant tuberin in which the ERK phospho-specific sites S540 and S664 have been mutated into aspartate (TSC2$^{S540D/S664D}$; TSC2-2D mutant) was unable to achieve the same effect, consistent with the ERK-dependent regulation of tuberin being responsible for the PC-1 effects.

From all these data, we conclude that PC-1 downregulates cell size and the mTOR pathway by affecting the ERK-mediated phosphorylation of tuberin at S664.

DISCUSSION

ADPKD is a slowly progressive disease characterized by renal cyst formation (38). Cysts generate from any segment of the renal tubule and expand in size and number throughout the life of an individual. Increased proliferation is one of the features observed in ADPKD cystic kidneys (11). In line with

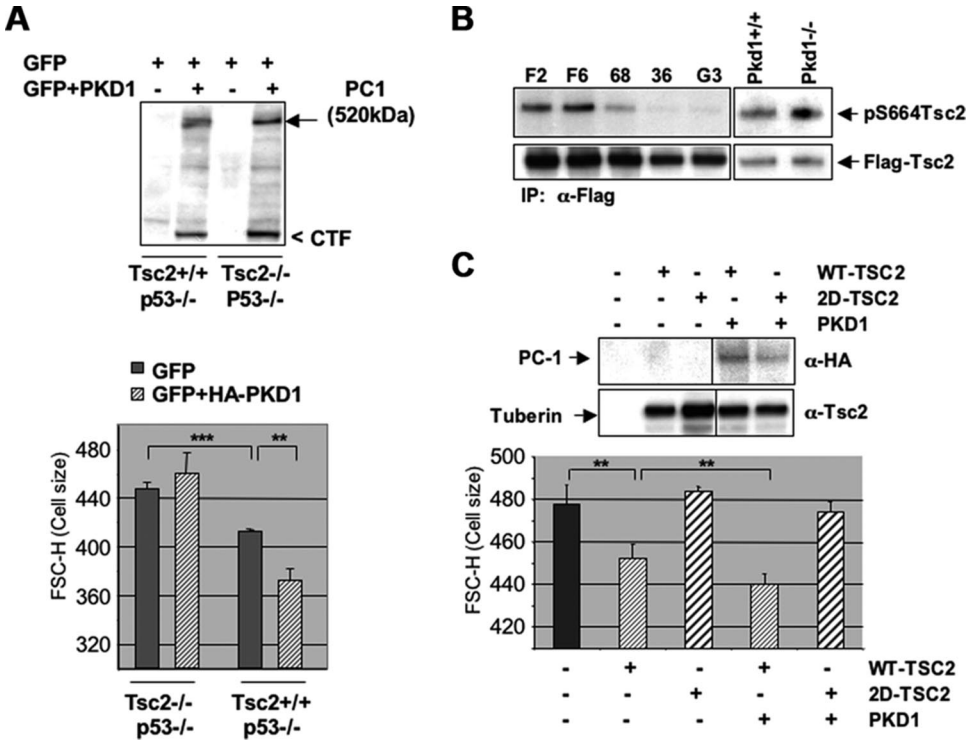

FIG. 8. PC-1 controls cell size and the mTOR pathway through regulation of tuberin phosphorylation in ERK-specific sites. (A) Transient transfection of GFP alone or in combination with a HA-*PKD1* construct performed in $Tsc2^{+/+}$; $p53^{-/-}$ or $Tsc2^{-/-}$; $p53^{-/-}$ MEFs. (Top) HA-*PKD1* was immunoblotted using anti-HA antibodies, revealing that equal expression levels for PC-1 are achieved in both cell lines. (Bottom) Statistical analysis of cell size quantification after synchronization in the G_0/G_1 phase of the cell cycle on triplicate transfections in $Tsc2^{+/+}$ and $Tsc2^{-/-}$ MEFs reveals that PC-1 induces a statistically significant reduction in cell size only in $Tsc2^{+/+}$ cells. Statistical analysis was performed by applying ANOVA (**, $P < 0.005$; ***, $P < 0.0001$). (B) Flag-tagged Tsc2 was transiently transfected in controls (F6 and F2), MDCK *PKD1* Zeo clones (C8/68 [68], G7/36 [36], and G3), and $Pkd1^{+/+}$ or $Pkd1^{-/-}$ MEFs, immunoprecipitated using anti-Flag antibodies (M2 beads), and immunoblotted using an anti-phospho-S664 antibody. Filters were then stripped and probed using an antituberin antibody as a loading control. A decrease in the phosphorylation levels of this site in all three MDCK *PKD1* Zeo cell lines was observed, while an increase occurred in the $Pkd1^{-/-}$ MEFs. (C) Transient transfection of wt tuberin into $Tsc2^{-/-}$; $p53^{-/-}$ cells decreases the size of cells, which is further enhanced by cotransfection of a *PKD1*-HA construct. (Top) Western blot analysis of tuberin and PC-1 (α-HA) in transiently transfected $Tsc2^{-/-}$; $p53^{-/-}$ cells at 48 h posttransfection. (Bottom) Analysis of triplicate experiments reveals that coexpression of PC-1 and wt-TSC2 results in a statistically significant reduction of cell size over that with transfection of wt-TSC2 alone. Statistical analysis was performed by applying ANOVA (**, $P < 0.005$). Transient transfection of $TSC2^{S540D/S664D}$ (2D-TSC2) is not able to affect cell size, neither when transfected alone nor when cotransfected with *PKD1*.

these findings, a direct role of PC-1 and -2 in regulating the cell cycle has been recently demonstrated and investigated in detail (2, 5, 22). In this report, we show that PC-1 controls cell growth (size) in addition to and independently of cell proliferation and that it does so through the Tsc/mTOR pathway and its downstream effectors p70S6K and 4EBP1. We show here that the overexpression of PC-1 in MDCK cells potently inhibits the Tsc/mTOR pathway, leading to reduced growth and size, and that MEFs lacking expression of the *Pkd1* gene have increased growth rates and increased activation of the Tsc/mTOR pathway.

Of great interest, a careful histological analysis of ADPKD cystic epithelia performed several years ago revealed that the mean surface area of the cells lining the cysts is largely increased compared to that of normal epithelia, although not to an extent sufficient to fully justify the increase in cyst size over the years (11). It was therefore proposed that a combination of proliferation and increased cell surface area accounts for the expansion of the cysts (11). While part of the increase in cell surface area might result from cell stretching in some of the cysts, it is difficult to imagine that this alone can justify the large extent of the described increase (where cells can acquire a cell surface area up to 15 times larger than normal). We propose that a combination of proliferation, stretching, and cellular hypertrophy (and possibly other, yet-unidentified factors) could all contribute to the increase in cyst size.

Notably, three recent reports have shown that the treatment of animal models of polycystic kidney disease with rapamycin results in a reduction of cyst volume (33, 35, 39). Although cellular hypertrophy was not evaluated in these mouse models, our data would suggest that the beneficial effects of rapamycin might be, at least in part, due to its ability to control cellular hypertrophy. In addition, the upregulation of the phosphorylation levels of p70S6K were reported in the cystic kidneys and livers of human tissues as well as in murine cystic kidneys (29, 33, 39), demonstrating that this pathway is misregulated in vivo.

Although the studies above have shown that the mTOR pathway is dysregulated in *PKD* mouse models, the molecular mechanisms leading to this were not investigated in detail.

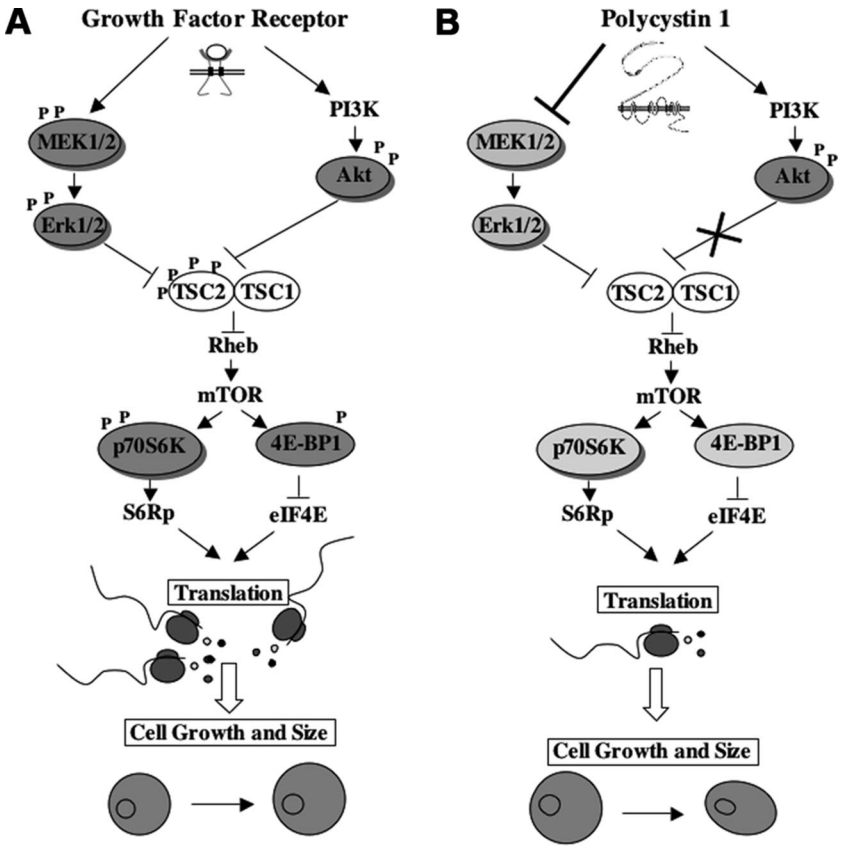

FIG. 9. Schematic representation of the proposed model. (A) Schematic representation of the dual mode of regulation of tuberin and the mTOR pathway in response to growth factors, as previously proposed by Ma et al. (24). Both the ERK and the Akt kinases can directly control the phosphorylation levels of tuberin, thus allowing for the double control of the pathway by growth factor receptors. (B) Proposed model for the regulation of the tuberin and mTOR pathway by PC-1. PC-1 induces activation of the PI3k/Akt pathway (3), but the pool of Akt activated in response to PC-1 is not able to phosphorylate Tsc2. At the same time, PC-1 overexpression downregulates the MEK/ERK pathway (our current work), resulting in reduced phosphorylation of tuberin and thus inhibition of mTOR. In ADPKD, the absence of PC-1 would result in the upregulation of the ERKs responsible for upregulating the mTOR pathway.

Shillingford et al. have shown that the overexpression of the short intracellular C-tail of PC-1 in MDCK cells results in the colocalization of this construct with tuberin in the Golgi compartment. Furthermore, it was shown that this short tail of PC-1 can interact with endogenous tuberin through coimmunoprecipitation studies. Based on this evidence, the authors proposed that PC-1 interaction with tuberin might somehow result in its activation and therefore in the inhibition of the mTOR pathway (33). Further studies will be required to definitively assess if full-length (and possibly endogenous) PC-1 interacts with tuberin under physiological conditions. However, assuming that PC-1 and tuberin interact, since a previous study had reported that tuberin is important for PC-1 trafficking to the plasma membrane, one alternative possibility is that the tuberin/PC-1 interaction might be important in that context (21). In this study, we demonstrate that PC-1 inhibits the mTOR signaling pathway through an unusual mechanism depending on ERK-dependent and Akt-independent regulation of the phosphorylation of tuberin. How this phosphorylation might impact the PC-1/tuberin interaction should be a matter of future investigation.

One question that remains open after our studies is how PC-1 regulates the ERK pathway. It was previously proposed that PC-1 might regulate the MEK/ERK cascade by regulating the phosphorylation status of B-Raf (41). In line with this work, our studies provide evidence that the overexpression of PC-1 can inhibit the MEK/ERK pathway and strongly suggest that this is a direct effect, since the opposite is observed in *Pkd1*$^{-/-}$ cells. A recent report has demonstrated that the inactivation of the *Pkd1* gene under controlled conditions in the kidney of *Pkd1* conditional knockout mice results in massive renal cystogenesis accompanied by increased activation of the ERK pathway (32), further suggesting a role for PC-1 in regulating this cascade. Shibazaki et al. also showed that treatment with low doses of the MEK inhibitor UO126 is not sufficient to revert cyst expansion despite being able to restore normal ERK phosphorylation (32). Several explanations can be provided for this apparent discrepancy with our results. These authors treated the mice by administering the MEK inhibitor every 3 days. While the biochemical effects on the phosphorylation levels of the ERKs were evaluated 24 h after treatment, the effect on cyst expansion was evaluated after a maximum time of 10 days (with the tolerated low doses of inhibitor) (32). However, the MEK inhibitor employed has a very short half-life and is quickly degraded in vivo. It is possible that in the 48 h between the time of measurement of the

phosphorylation levels of the ERKs and the next administration of the inhibitor, the ERK pathway and consequently the mTOR are restored in the cystic epithelia. This alternation of inhibition and hyperactivation of the MEK/ERK pathway might not be sufficient to prevent cyst expansion. Using a less-degradable compound, and perhaps combining low doses of both rapamycin and a Raf or MEK inhibitor, might help prevent cyst expansion. A similar combination of drugs was shown to be beneficial in the treatment of melanoma (26).

Finally, we cannot exclude the possibility that additional feedback loops and additional activating molecules are converging on the mTOR pathway in vivo and might be acting synergistically to enhance mTOR activity. Interestingly, the Wnt pathway, previously shown to be regulated by PC-1 (20), is also able to act on the mTOR cascade via AMPK and GSK3β, and this might contribute to the enhanced mTOR activity in cystic epithelia (16). Since we have previously demonstrated that PC-1 can enhance the activity of GSK3β (4), we cannot exclude the possibility that this alternative pathway will play a role in regulating the mTOR pathway under conditions of nutrient deprivation or hypoxia, both of which are likely to occur in vivo as cysts expand over time.

We believe that one of the most important aspects of our work is delineation of the mechanism of regulation of the mTOR pathway by PC-1. We have demonstrated that PC-1 can downregulate the mTOR pathway through direct regulation of the ERK-specific phospho-sites on tuberin (serine 664), through a mechanism recently described (24). We propose that PC-1, a non-tyrosine kinase receptor, might enable the distinguishing of Akt-dependent and ERK-dependent regulation of tuberin and the studying of the two processes separately (model proposed in Fig. 9). Although our data demonstrate that the ERK pathway is the major regulator of mTOR in response to PC-1, it remains to be elucidated why active Akt alone is not sufficient to achieve activation of the mTOR pathway. With respect to this point, it is important to highlight that the Ser/Thr kinase mTOR can be observed in at least two distinct functional complexes: the mTORC1 and the mTORC2 (40). The mTORC2 complex is the kinase that phosphorylates Akt in Ser473. It appears from our data that the mTORC1 complex is inhibited by PC-1, while the mTORC2 is activated. In our cell system, Akt is not able to phosphorylate tuberin despite the fact that Akt is fully active, as demonstrated by its phosphorylation at both Ser473 and Thr308 and by its capability to phosphorylate another downstream effector, FKHR (or FOXO) (3). Interestingly, several recent reports have shown that the knockout of the mTORC2 complex in vivo completely abolishes the phosphorylation of Akt at Ser473, demonstrating that this complex is responsible for the phosphorylation of this site in vivo (12, 18, 34). Surprisingly, the lack of Akt phosphorylation at Ser473 results in impaired phosphorylation of the forkhead transcription factor FOXO but not of tuberin nor of GSK3β (12, 18, 34). Similarly, in our model system, active Akt phosphorylates the forkhead transcription factor FKHR (3) but not GSK3β (4) or TSC2 (the current work). In addition, a new component of the mTORC2 complex, SIN, was shown to regulate the specificity of the substrates phosphorylated by Akt (18). Furthermore, it was reported that SIN1 exists in several different isoforms, each of which can associate with the TORC2 complex (10). It was proposed that these different isoforms generate several different forms of mTORC2 that act on different pools of cellular Akt and thus determine the specificity of Akt action on its substrates (10). In light of these findings, our results are not surprising but rather highlight the intriguing possibility that PC-1 might be able to differentially regulate the activity of the mTORC1 and mTORC2 complexes.

ACKNOWLEDGMENTS

We are grateful to the other members of the Boletta lab for helpful discussions; M. Chiaravalli and V. Basso for technical help; S. Biffo and R. Bernardi for critically reading the manuscript; F. Qian, S. Ahn, C. Z. Chen, M. E. Greenberg, R. A. Roth, and J. Blenis for kindly providing HA-*PKD1*, CA-MEK, wt-p70S6K, wt- and DN-Akt, CA-Akt, and eIF4E constructs, respectively; D. Kwiatkowski for the $Tsc2^{+/+}$ and $Tsc2^{-/-}$ MEFs; and A. De Marco for providing the TATCre.

G.G.G. and K.B.P. are supported by NIH DK R37 48006. G.G.G. is the Irving Blum Scholar of the Johns Hopkins University School of Medicine. P.P.P. and L.M. are supported by NIH/NCI CA84292. A.B. is a Marie Curie Excellence Team Leader supported by the European Community (MCEXT-CT-2003-002785) and by Telethon-Italy (TCP01018) and is an Associate Telethon Scientist.

REFERENCES

1. **Ballif, B. A., P. P. Roux, S. A. Gerber, J. P. MacKeigan, J. Blenis, and S. P. Gygi.** 2005. Quantitative phosphorylation profiling of the ERK/p90 ribosomal S6 kinase-signaling cassette and its targets, the tuberous sclerosis tumor suppressors. Proc. Natl. Acad. Sci. USA **102:**667–672.
2. **Bhunia, A. K., K. Piontek, A. Boletta, L. Liu, F. Qian, P. N. Xu, F. J. Germino, and G. G. Germino.** 2002. *PKD1* induces p21(waf1) and regulation of the cell cycle via direct activation of the JAK-STAT signaling pathway in a process requiring *PKD2*. Cell **109:**157–168.
3. **Boca, M., G. Distefano, F. Qian, A. K. Bhunia, G. G. Germino, and A. Boletta.** 2006. Polycystin-1 induces resistance to apoptosis through the phosphatidylinositol 3-kinase/Akt signaling pathway. J. Am. Soc. Nephrol. **17:** 637–647.
4. **Boca, M., L. D'Amato, G. Distefano, R. S. Polishchuk, G. G. Germino, and A. Boletta.** 2007. Polycystin-1 induces cell migration by regulating PI3kinase-dependent cytoskeletal rearrangements and GSK3-β dependent cell cell mechanical adhesion. Mol. Biol. Cell **18:**4050–4061.
5. **Boletta, A., F. Qian, L. F. Onuchic, A. K. Bhunia, B. Phakdeekitcharoen, K. Hanaoka, W. Guggino, L. Monaco, and G. G. Germino.** 2000. Polycystin-1, the gene product of *PKD1*, induces resistance to apoptosis and spontaneous tubulogenesis in MDCK cells. Mol. Cell **6:**1267–1273.
6. **Boletta, A., and G. G. Germino.** 2003. Role of polycystins in renal tubulogenesis. Trends Cell Biol. **13:**484–492.
7. **Cai, S. L., A. R. Tee, J. D. Short, J. M. Bergeron, J. Kim, J. Shen, R. Guo, C. L. Johnson, K. Kiguchi, and C. L. Walker.** 2006. Activity of TSC2 is inhibited by AKT-mediated phosphorylation and membrane partitioning. J. Cell Biol. **173:**279–289.
8. **Conlon, I., and M. Raff.** 24 April 2003. Differences in the way a mammalian cell and yeast cells coordinate cell growth and cell-cycle progression. J. Biol. **2:**7. [Epub ahead of print.]
9. **Fingar, D. C., S. Salama, C. Tsou, E. Harlow, and J. Blenis.** 2002. Mammalian cell size is controlled by mTOR and its downstream targets S6K1 and 4EBP1/eIF4E. Genes Dev. **16:**1472–1487.
10. **Frias, M. A., C. C. Thoreen, J. D. Jaffe, W. Schroder, T. Sculley, C. A. Carr, and D. M. Sabatini.** 2006. mSin1 is necessary for Akt/PKB phosphorylation, and its isoforms define three distinct mTORC2s. Curr. Biol. **16:**1865–1870.
11. **Grantham, J. J., J. L. Geiger, and A. P. Evan.** 1987. Cyst formation and growth in autosomal dominant polycystic kidney disease. Kidney Int. **31:** 1145–1152.
12. **Guertin, D. A., D. M. Stevens, C. C. Thoreen, A. A. Burds, N. Y. Kalaany, J. Moffat, M. Brown, K. J. Fitzgerald, and D. M. Sabatini.** 2006. Ablation in mice of the mTORC components raptor, rictor, or mLST8 reveals that mTORC2 is required for signaling to Akt-FOXO and PKCalpha, but not S6K1. Dev. Cell **11:**859–871.
13. **Hanaoka, K., F. Qian, A. Boletta, A. K. Bhunia, K. Piontek, L. Tsiokas, V. P. Sukhatme, W. B. Guggino, and G. G. Germino.** 2000. Co-assembly of polycystin-1 and -2 produces unique cation-permeable currents. Nature **408:**990–994.
14. **Hsu, Y. C., J. J. Chern, Y. Cai, M. Liu, and K. W. Choi.** 2007. Drosophila TCTP is essential for growth and proliferation through regulation of dRheb GTPase. Nature **445:**785–788.
15. **Ibraghimov-Beskrovnaya, O., N. O. Bukanov, L. C. Donohue, W. R. Dack-**

owski, K. W. Klinger, and G. M. Landes. 2000. Strong homophilic interactions of the Ig-like domains of polycystin-1, the protein product of an autosomal dominant polycystic kidney disease gene, *PKD1*. Hum. Mol. Genet. **9:**1641–1649.
16. **Inoki, K., H. Ouyang, T. Zhu, C. Lindvall, Y. Wang, X. Zhang, Q. Yang, C. Bennett, Y. Harada, K. Stankunas, C. Y. Wang, X. He, O. A. MacDougald, M. You, B. O. Williams, and K. L. Guan.** 2006. TSC2 integrates Wnt and energy signals via a coordinated phosphorylation by AMPK and GSK3 to regulate cell growth. Cell **126:**955–968.
17. **Inoki, K., T. Zhu, and K. L. Guan.** 2003. TSC2 mediates cellular energy response to control cell growth and survival. Cell **115:**577–590.
18. **Jacinto, E., V. Facchinetti, D. Liu, N. Soto, S. Wei, S. Y. Jung, Q. Huang, J. Qin, and B. Su.** 2006. SIN1/MIP1 maintains rictor-mTOR complex integrity and regulates Akt phosphorylation and substrate specificity. Cell **127:**125–137.
19. **Joshi, S. K., K. Hashimoto, and P. A. Koni.** 2002. Induced DNA recombination by Cre recombinase protein transduction. Genesis **33:**48–54.
20. **Kim, E., T. Arnould, L. K. Sellin, T. Benzing, M. J. Fan, W. Grüning, S. Y. Sokol, I. Drummond, and G. Walz.** 1999. The polycystic kidney disease 1 gene product modulates Wnt signaling. J. Biol. Chem. **274:**4947–4953.
21. **Kleymenova, E., O. Ibraghimov-Beskrovnaya, H. Kugoh, J. Everitt, H. Xu, K. Kiguchi, G. Landes, P. Harris, and C. Walker.** 2001. Tuberin-dependent membrane localization of polycystin-1: a functional link between polycystic kidney disease and the TSC2 tumor suppressor gene. Mol. Cell **7:**823–832.
22. **Li, X., Y. Luo, P. G. Starremans, C. A. McNamara, Y. Pei, and J. Zhou.** 2005. Polycystin-1 and polycystin-2 regulate the cell cycle through the helix-loop-helix inhibitor Id2. Nat. Cell Biol. **7:**1102–1112.
23. **Ma, L., J. Teruya-Feldstein, P. Bonner, R. Bernardi, D. N. Franz, D. Witte, C. Cordon-Cardo, and P. P. Pandolfi.** 2007. Identification of S664 TSC2 phosphorylation as a marker for extracellular signal-regulated kinase mediated mTOR activation in tuberous sclerosis and human cancer. Cancer Res. **67:**7106–7112.
24. **Ma, L., Z. Chen, H. Erdjument-Bromage, P. Tempst, and P. P. Pandolfi.** 2005. Phosphorylation and functional inactivation of TSC2 by Erk implications for tuberous sclerosis and cancer pathogenesis. Cell **121:**179–193.
25. **Manning, B. D., A. R. Tee, M. N. Logsdon, J. Blenis, and L. C. Cantley.** 2002. Identification of the tuberous sclerosis complex-2 tumor suppressor gene product tuberin as a target of the phosphoinositide 3-kinase/akt pathway. Mol. Cell **10:**151–162.
26. **Molhoek, K. R., D. L. Brautigan, and C. L. Slingluff, Jr.** 2005. Synergistic inhibition of human melanoma proliferation by combination treatment with B-Raf inhibitor BAY43-9006 and mTOR inhibitor rapamycin. J. Transl. Med. **3:**39.
27. **Pan, D., J. Dong, Y. Zhang, and X. Gao.** 2004. Tuberous sclerosis complex: from Drosophila to human disease. Trends Cell Biol. **14:**78–85.
28. **Qian, F., F. J. Germino, Y. Cai, X. Zhang, S. Somlo, and G. G. Germino.** c1997. PKD1 interacts with PKD2 through a probable coiled-coil domain. Nat. Genet. **16:**179–183.
29. **Qian, Q., H. Du, B. F. King, S. Kumar, P. G. Dean, F. G. Cosio, and V. E. Torres.** 2008. Sirolimus reduces polycystic liver volume in ADPKD patients. J. Am. Soc. Nephrol. **19:**631–638.
30. **Roux, P. P., B. A. Ballif, R. Anjum, S. P. Gygi, and J. Blenis.** 2004. Tumor-promoting phorbol esters and activated Ras inactivate the tuberous sclerosis tumor suppressor complex via p90 ribosomal S6 kinase. Proc. Natl. Acad. Sci. USA **101:**13489–13494.
31. **Ruvinsky, I., and O. Meyuhas.** 2006. Ribosomal protein S6 phosphorylation: from protein synthesis to cell size. Trends Biochem. Sci. **31:**342–348.
32. **Shibazaki, S., Z. Yu, S. Nishio, X. Tian, R. B. Thomson, M. Mitobe, A. Louvi, H. Velazquez, S. Ishibe, L. G. Cantley, P. Igarashi, and S. Somlo.** 2008. Cyst formation and activation of the extracellular regulated kinase pathway after kidney specific inactivation of *Pkd1*. Hum. Mol. Genet. **17:**1505–1516.
33. **Shillingford, J. M., N. S. Murcia, C. H. Larson, S. H. Low, R. Hedgepeth, N. Brown, C. A. Flask, A. C. Novick, D. A. Goldfarb, A. Kramer-Zucker, G. Walz, K. B. Piontek, G. G. Germino, and T. Weimbs.** 2006. The mTOR pathway is regulated by polycystin-1, and its inhibition reverses renal cystogenesis in polycystic kidney disease. Proc. Natl. Acad. Sci. USA **103:**5466–5471.
34. **Shiota, C., J. T. Woo, J. Lindner, K. D. Shelton, and M. A. Magnuson.** 2006. Multiallelic disruption of the rictor gene in mice reveals that mTOR complex 2 is essential for fetal growth and viability. Dev. Cell **11:**583–589.
35. **Tao, Y., J. Kim, R. W. Schrier, and C. L. Edelstein.** 2005. Rapamycin markedly slows disease progression in a rat model of polycystic kidney disease. J. Am. Soc. Nephrol. **16:**46–51.
36. **Tee, A. R., B. D. Manning, P. P. Roux, L. C. Cantley, and J. Blenis.** 2003. Tuberous sclerosis complex gene products, Tuberin and Hamartin, control mTOR signaling by acting as a GTPase-activating protein complex toward Rheb. Curr. Biol. **13:**1259–1268.
37. **Tee, A. R., and J. Blenis.** 2005. mTOR, translational control and human disease. Semin. Cell Dev. Biol. **16:**29–37.
38. **Torres, V. E., P. C. Harris, and Y. Pirson.** 2007. Autosomal dominant polycystic kidney disease. Lancet **369:**2157.
39. **Wahl, P. R., A. L. Serra, M. Le Hir, K. D. Molle, M. N. Hall, and R. P. Wuthrich.** 2006. Inhibition of mTOR with sirolimus slows disease progression in Han:SPRD rats with autosomal dominant polycystic kidney disease (ADPKD). Nephrol. Dial. Transplant. **21:**598–604.
40. **Wullschleger, S., R. Loewith, and M. N. Hall.** 2006. TOR signaling in growth and metabolism. Cell **124:**471–484.
41. **Yamaguchi, T., D. P. Wallace, B. S. Magenheimer, S. J. Hempson, J. J. Grantham, and J. P. Calvet.** 2004. Calcium restriction allows cAMP activation of the B-Raf/ERK pathway, switching cells to a cAMP-dependent growth-stimulated phenotype. J. Biol. Chem. **279:**40419–40430.